Selective adsorption of toluene-3,4-dithiol on Si(553)-Au surfaces

Svetlana Suchkova,[1] Conor Hogan,[2,*] Friedhelm Bechstedt,[3] Eugen Speiser,[1] and Norbert Esser[1]
[1]*Leibniz-Institut für Analytische Wissenschaften-ISAS-e.V., Schwarzschildstraße 8, 12489 Berlin, Germany*
[2]*Istituto di Struttura della Materia-CNR, Via del Fosso del Cavaliere, 00133 Rome, Italy*
[3]*Institut für Festkörpertheorie und -optik, Friedrich-Schiller-Universität Jena, Max-Wien-Platz 1, 07743 Jena, Germany*

(Received 19 September 2017; published 17 January 2018)

The adsorption of small organic molecules onto vicinal Au-stabilized Si(111) surfaces is shown to be a versatile route towards controlled growth of ordered organic-metal hybrid one-dimensional nanostructures. Density functional theory is used to investigate the site-specific adsorption of toluene-3,4-dithiol (TDT) molecules onto the clean Si(553)-Au surface and onto a co-doped surface whose steps are passivated by hydrogen. We find that the most reactive sites involve bonding to silicon at the step edge or on the terraces, while gold sites are relatively unfavored. H passivation and TDT adsorption both induce a controlled charge redistribution within the surface layer, causing the surface metallicity, electronic structure, and chemical reactivity of individual adsorption sites to be substantially altered.

DOI: 10.1103/PhysRevB.97.045417

I. INTRODUCTION

Organic functionalization of semiconductors is an important route towards the development of novel semiconductor-based devices in optoelectronics and sensor technology. In particular on silicon surfaces quite a lot of related work has been published in recent years [1–4]. The self-organization of organic molecules is a promising bottom-up approach in contrast to further downscaling lithographic techniques for device manufacturing. The critical issue is, however, to control the chemical interaction of the molecules with the surface which governs the structure formation. In contrast to metal surfaces where a weak molecule-substrate interaction allows molecules to diffuse and arrange according to molecular interaction, on semiconductors a strong molecule-substrate interaction arises from covalent bonding. Thus, the formation of molecular structures has to be controlled by the local surface reactivity with the impinging molecules.

Silicon, being a covalent semiconductor, provides various adsorption paths for organic molecules. Such paths include H abstraction and covalent bonding between a Si dangling bond (DB) and the molecule, as well as Diels-Alder reactions involving C–C and Si–Si double bonds of the molecules and the surface, respectively. Benzene (C_6H_6) and toluene (C_7H_8) are examples of unsaturated aromatic hydrocarbons whose adsorption on Si surfaces has been intensively examined in recent years. Toluene differs from benzene only by the presence of a methyl group, $-CH_3$, as a substituent of the ring. The methyl group alters the adsorption properties of benzene on Si surfaces dramatically [4,5]. Other side groups may dramatically modify the deposition of organic molecules further.

The interaction of organic molecules with metal surfaces appears much simpler. A very well known example concerns molecules with thiol $-$SH end groups [3] on gold surfaces, where it is well established that S–Au bonds underpin the molecule-substrate interaction. Examples are the formation of self-assembled monolayers (SAMs) of thiol-modified alkanes on gold [6,7] and the cysteine adsorption on Au(110) surfaces (see Ref. [8] and references therein).

Thus, for generating a well-defined and ordered molecule-Si-interface a promising approach could be the use of metal-adsorbate-modified Si surfaces as a template, such as the Au atomic nanostructures formed on Si surfaces. One-dimensional atomic gold chains are known to form by self-assembly on vicinal Si(111) surfaces and act to stabilize their geometry over long distances [9–12]. These metallic chains constitute possible templates for the interaction with organic molecules aimed at the formation of regular, ordered patterns of organic-metal hybrid nanostructures [13]. The Au chain structure can be easily tuned by varying the vicinal angle (single, double, and triple atomic chains have been prepared [14]) and gives rise to interesting physical properties (Peierls transitions, spin chains) that are currently the subject of intensive research [11,15]. Such one-dimensional (1D) Au–Si nanostructures as a template for organic SAM growth represent a quite attractive substrate choice, as they may even yield unique chemical and physical properties due to the hybridization of the 1D metallic states with the organic π-conjugated molecules.

Although many studies of SAMs on Au surfaces and on clean and stepped Si surfaces have been performed (the potential of stepped Si for growing nanostructure arrays has long been noted [9]), only a handful of experimental works have been done on surface-supported atomic Au wires of this type [13,16]. On the theoretical side, atomic adsorption of various species [e.g., Ag, Pb, and O adsorption on Si(553)-Au [17,18]] has been studied with density functional theory (DFT), but as yet, organic molecules have hardly been investigated.

In this work we study the adsorption of toluene-3,4-dithiol (TDT) on the vicinal Si(553)-Au surface. This is a rigid aromatic divalent thiol having two $-$SH ligands. We focus

*Author to whom correspondence should be addressed: conor.hogan@ism.cnr.it

on site specificity as an order control parameter, rather than intermolecular coupling. By means of DFT calculations [19,20] we investigate energetics, geometry, and electronic properties of such hybrid interfaces on Si(553)-Au. Furthermore, we investigate adsorption on a Au/Si surface whose local reactivity has been changed through prepassivation by atomic hydrogen.

The methodology and the numerical approach is presented in Sec. II. As a first step the adsorption of an isolated thiolate group is studied in Sec. III in order to find the most favorable bonding sites for the TDT molecules, and different adsorption channels are investigated. In a second step (Sec. IV) a full structural relaxation of the TDT molecules is performed for adsorption at minimum energy sites, and the structure and electronic interface properties are derived. This procedure is applied for Si(553)-Au surfaces with and without hydrogen passivation of Si dangling bonds at the step edge. The paper concludes with a summary and outlook of possible future applications of our approach (Sec. V).

II. METHODOLOGY

First-principles calculations of the geometry and electronic structure were performed using density functional theory as implemented in the plane-wave/pseudopotential code QUANTUM ESPRESSO [21]. Norm-conserving pseudopotentials were used along with a kinetic-energy cutoff of 65 Ry. Geometry optimizations were performed using the Broyden-Fletcher-Goldfarb-Shanno [22] algorithm. During structural relaxation, forces were converged according to a (low) threshold of 12 meV/Å. Spin polarization [11] is not taken into account. The investigated adsorption mechanisms and sites are usually related to paired electrons.

Surfaces were modeled using (1×4) supercells composed of Si diamond slabs (five Si bilayers thick, about 15 Å) separated by thick vacuum regions (28 Å) [23]. This facilitates a minimum vacuum thickness of 20 Å after molecule adsorption perpendicular to the surface. The back surface was passivated by hydrogen and held fixed to simulate the Si bulk. The oblique lateral (1×1) unit cell is spanned by a basis vector, $\vec{a}_2$, in the $[1\bar{1}0]$ direction and another one, $\vec{a}_1$, in the $[11\bar{2}]$ direction with two Au atoms and seven Si atoms in the surface layer. To allow for dimerization of Au atoms in the $[1\bar{1}0]$ direction, (1×2) reconstructions are studied. The corresponding basic model in Fig. 1(a) was proposed by Krawiec [24]. The dimerized double Au chains lying on the (553) terraces and silicon honeycomb structures at the step edges are clearly visible. In order to avoid intermolecular interactions, we consider (1×4) cells [11] (double the basic periodicity determined by the Au chain dimerization). With this large cell size, we find that Γ-point-only Brillouin zone (BZ) sampling is sufficient and yields absolute adsorption energies converged to 0.1 eV and relative energies better than 0.01 eV, i.e., small compared to other methodological errors.

The exchange-correlation (XC) functional of the DFT is modeled using the local-density approximation (LDA) [25], which gives an adequate description of charge transfer, chemical bonding, and surface geometries in many semiconductor/adsorbate systems. The LDA is well known to overbind in layered materials and metallo-organic systems and lacks a proper treatment of van der Waals (vdW) correlation. Nonetheless, due to its overestimation of exchange, it has sometimes been used as a poor replacement for vdW interactions. For these reasons, we consider only chemisorbed geometries with strong mixed ionic-covalent bonds, e.g., formation of almost covalent S–Si or S–Au bonds, typically following dissociation of thiol (−SH) groups. A numerical justification of our choice of LDA is given in the Appendix.

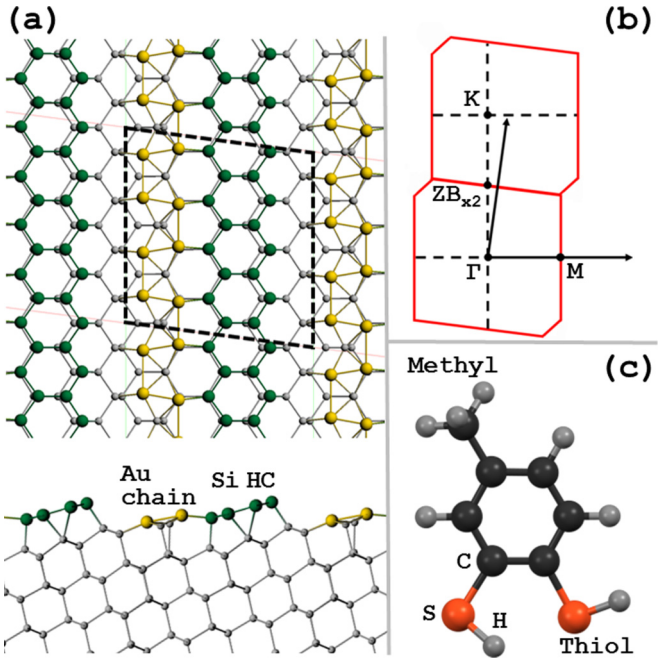

FIG. 1. (a) Schematic structure of the clean Si(553)-Au surface. Only the topmost layers are shown. The Au (Si) atoms are represented by yellow (green) circles. The dashed lines indicate a (1×4) surface unit cell. (b) The (1×4) surface Brillouin zone is shown by red lines. High-symmetry points Γ, K, and M are shown. K corresponds to the zone boundary of the (1×2) surface. (c) Toluene-3,4-dithiol (TDT). The C, S, and H atoms are represented by dark gray, red-orange, and light gray circles, respectively.

III. ADSORPTION SITES AND MECHANISMS

A. Thiol ligand adsorption

According to our calculations, the TDT molecule tries to bond to the Si(553)-Au surface via its very reactive thiol side groups but not via the methyl head group of toluene. We thus investigate in the first step the adsorption of the thiol ligand (more strictly speaking, of thiolate) without the toluene molecule in order to identify the most energetically favorable adsorption sites. This will then help us to determine the likely adsorption sites and orientations of the larger TDT molecule.

A methanethiolate side group ($-S-CH_3$) is chosen to simulate surface adsorption of the S linker. We reduce the parameter space by computing the potential-energy surface (PES) for methanethiolate adsorption across the clean Si(553)-Au surface over a large (1×4) cell. The results are displayed as a contour map in Fig. 2(a). In calculating the PES, the lateral position of the $-S-CH_3$ group is fixed at a certain (x, y) coordinate in the xy plane, while its position (z) in

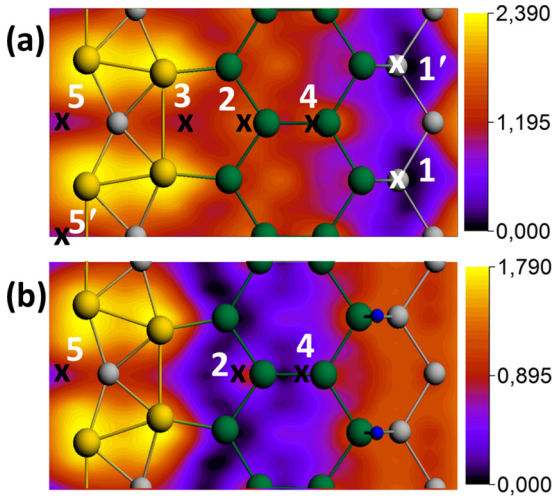

FIG. 2. Potential-energy surface for methanethiolate adsorption on (a) clean and (b) step-edge-passivated Si(553)-Au. The color scale indicates energies in eV relative to the global minimum. The Au, bulk Si, honeycomb Si, and H atoms of the surface unit cell are indicated in gold, light gray, green, and blue, respectively. Crosses label specific adsorption sites after full relaxation (see text).

the surface-normal direction is optimized by minimizing the total energy. The top two surface layers are allowed to relax. The calculation is then repeated across a regular grid of (x, y) coordinates in the surface cell. Adsorption on the Au bridge site 5 is found to induce a phase shift in the Au dimerization, such that sites 5 and 5′ are equivalent. Instead, adsorption at DB sites 1 and 1′ differ by 3.6 meV due to the $\times 2$ periodicity of the Au chains. As this difference is negligible on the scale of the plot, we computed total energies over only one quarter of the (1×4) simulation cell. The PES computed over the true (1×2) periodicity would appear slightly less symmetric [26]. Energies in Fig. 2(a) are plotted relative to the absolute minimum energy found. Pronounced minima and maxima are observed. Most interesting are Si$-$S$-$CH$_3$ and Au$-$S$-$CH$_3$ bonds. The step edge dangling bond is by far the most stable site for adsorption of methanethiolate, similar to studies of hydrogen adsorption performed elsewhere on clean Si(553)-Au [27]. In contrast, binding to Au, with possible formation of Au chain/organic hybrids, appears to be naturally unfavored.

To refine the adsorption energies near the most stable adsorption sites, we then allowed the $-$S$-$CH$_3$ group to freely relax, in particular allowing it to tilt and rotate. The most favored sites identified in this way are marked by crosses in Fig. 2. The dangling bond site 1 remains the lowest-energy site, while other preferred sites lie closer in energy. Two possible sites lie at the Si=Si double bond of the honeycomb, with energies 2 = 0.612 eV and 4 = 0.641 eV with respect to 1. Other sites of similar energy lie in bridging positions on the Au chains: 3 = 0.624 eV and 5 = 0.661 eV.

We next investigate the possibility of "switching off" the reactivity of the edge states 1 by passivating them with hydrogen. Hydrogen, whether in the molecular phase or the atomic phase, will readily react with the step edge and passivate the dangling bonds [27]. The relative reactivity of adsorption sites on the terraces and Au chains should then be increased. We thus repeated the PES calculation but using a Si(553)-Au substrate with completely passivated step edge states (sites 1 occupied). For brevity, we will herein refer to this surface as the "passivated" surface (this usage will be justified in Sec. IV C). As shown in Fig. 2(b), the potential-energy landscape indeed changes significantly. Adsorption is now strongly confined to the Si honeycomb region. With respect to the most stable site on the passivated surface (2), site 4 is relatively accessible at 4 = 0.117eV, whereas the Au bridge sites now appear to be completely unreactive: 5 = 0.798 eV, and 3 is no longer a local minimum.

Based on these results, we conclude that the step edge dangling bond site 1 is by far the most stable adsorption site for sulfur ligands. After step edge passivation by H, the Si honeycomb sites on the terrace dominate the adsorption behavior. Thus, although S–Au bonds frequently occur on pure Au surfaces [6,8] and form the basis of many metallo-organic SAMs, here S–Si bonds are overwhelmingly favored. Even if the DBs are passivated, the molecule with a thiol ligand will prefer to bond on the double bonds of the Si honeycomb structure rather than on the Au chains. While S-terminated molecules readily bind to pure Au surfaces, they do not tend to bind to Au present on Si surfaces due to the presence of highly reactive Si DBs. The metal Au chains have only an indirect influence on adsorption via their stabilization of the stepped surface structure.

B. Molecular adsorption channels and the role of hydrogen

Having identified the most likely adsorption sites for the S linker, we consider the adsorption mechanism of the full TDT molecule. As noted above, TDT has two very reactive thiol side groups. In the following we assume that adsorption occurs via chemical bonding of *both* thiol ligands with the surface. This finding allows us to attack better the difficult problem as many atomic configurations are possible. We also note that the interatomic distance between the two S atoms (∼3.3 Å) is not far from the distance between adjacent favored sites along the $[1\bar{1}0]$ direction (∼3.8 Å, i.e., $a_0/\sqrt{2}$, with a_0 being the bulk Si lattice constant). Thus, it is particularly important to consider adsorption of TDT parallel to the step edge, including at adjacent Si DB sites.

Before tackling this problem in Sec. IV, we first investigate the role of the hydrogen atoms during the adsorption of the thiol (–SH) groups, which has not been considered up to now. We focus on three possible mechanisms (channels) for adsorption of a single TDT molecule on a (1×4) cell of Si(553)-Au. These channels are depicted in Fig. 3.

The first channel, channel (i), describes *dithiolate* adsorption with formation of S–Si and/or S–Au bonds, following S–H bond dissociation and release of H_2 into the rest gas. The adsorption energy is described by

$$E_{\text{ads}}^{(\text{i})} = -\left(E_{(1\times4)+\text{TDT}'} + E_{\text{H}_2} - E_{(1\times4)} - E_{\text{TDT}}\right). \quad (1)$$

Here $E_{(1\times4)}$ is the total energy of the clean surface, $E_{(1\times4)+\text{TDT}'}$ is the total energy of the surface with adsorbed dithiolate (TDT′), E_{TDT} is the energy of the undissociated dithiol, and E_{H_2} is the energy of an isolated H_2 molecule. In this way, we assume reservoirs of noninteracting TDT and H_2 molecules.

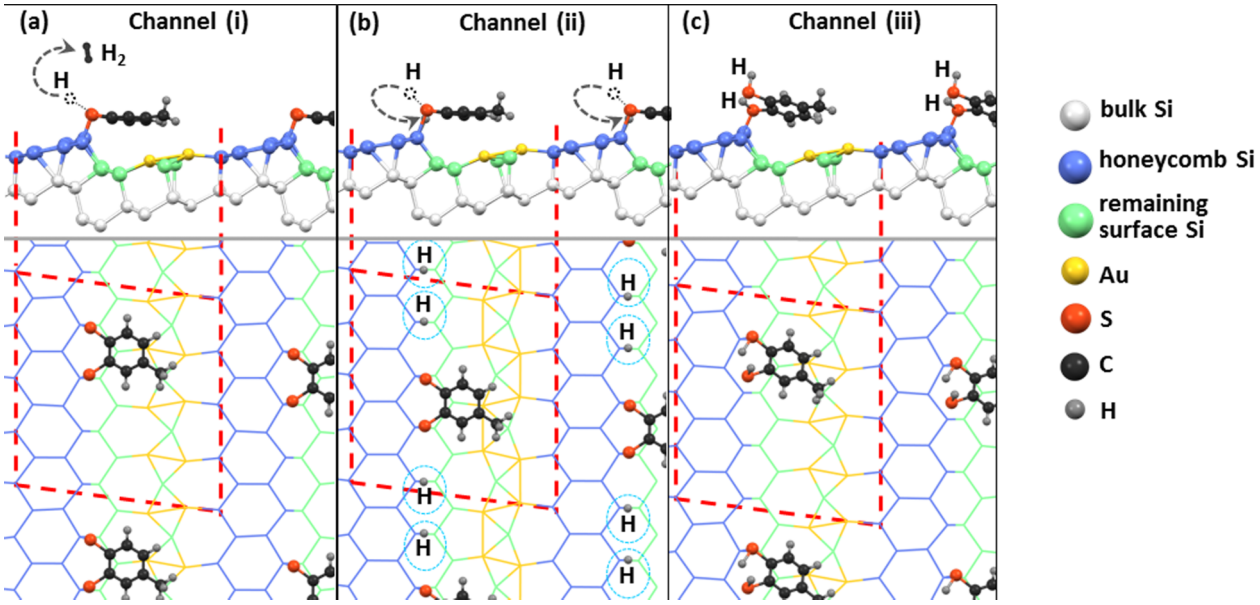

FIG. 3. Adsorption geometries of TDT on Si(553)-Au (top and side views). Possible reactions of the H atoms in the −SH groups during the adsorption process are illustrated. The dashed red lines indicate the (1 × 4) surface unit cell used in the simulations.

In a second channel, channel (ii), dithiolate adsorption again occurs, but in this case the two H atoms from the thiol groups passivate two of the step edge dangling bonds. Thus, it holds that

$$E_{\text{ads}}^{(\text{ii})} = -(E_{(1\times4):2\text{H}+\text{TDT}'} - E_{(1\times4)} - E_{\text{TDT}}). \quad (2)$$

Here $E_{(1\times4):2\text{H}}$ indicates that two H atoms are adsorbed on the step edge dangling bond sites of the (1 × 4) cell.

A third channel, channel (iii) describes a mechanism in which S–H dissociation does not occur. The full dithiol adsorbs via C–(H)S–Si/Au bonds. The adsorption energy is thus defined as

$$E_{\text{ads}}^{(\text{iii})} = -(E_{(1\times4)+\text{TDT}} - E_{(1\times4)} - E_{\text{TDT}}). \quad (3)$$

The resulting adsorption energies are reported in Table I. Channel (ii) is clearly the most energetically favorable one since it includes passivation of the surface dangling bonds by H. This process assumes sites are always available and hence is valid mostly for low coverages. The energy gain due to the formation of strong S–Si bonds and two H-Si bonds at the edges overcomes the energy lost through dissociation of two H–S bonds. Furthermore, the adsorption process assumes that any dissociation and H hopping barriers can be overcome, and H_2 formation is avoided. All DB sites in the (1 × 4) cell are passivated, which stabilizes the adsorbate structure. Thus, when step edge sites are available, this channel should be considered. Hydrogen adsorption at the step edge could well be a limiting factor in the growth of SAMs at the step. The smaller energy gain of channel (i) indicates that the two H-Si bonds are stronger than the bonding in diatomic H_2. Notably, channel (iii), i.e., intact thiol adsorption, appears to be unfavored. This is in strong contrast to adsorption on the Ag(111) surface, where the difference in binding energy between thiol and thiolate adsorption was reported to be less than 0.1 eV [28].

In order to avoid these issues while comparing different adsorption sites, in the following we consider only channel (i); that is, we assume H_2 formation and adsorption of the dithiolate species.

TABLE I. Adsorption energies (in eV) corresponding to different channels for TDT adsorption.

Channel	E_{ads}
(i) H_2 release	2.80
(ii) H passivation of step edge	4.43
(iii) No S–H dissociation	1.64

IV. MOLECULAR ADSORPTION

A. Geometry and energetics: Clean surface

Guided by the results of Sec. III A, we now consider TDT adsorption on the clean Si(553)-Au surface for a variety of possible adsorption sites. Characteristic adsorption energies, computed using Eq. (1), are reported alongside the various adsorbate structures in Fig. 4. Adsorption is depicted on the Si steps (structures A and B), on the Si honeycomb (HC) stripes (structure C), on the Au chains (structure D), and on a mixed Au chain/HC site (structure E).

As anticipated from our study with the methanethiolate group, the step edge dangling bonds offer by far the most reactive sites. Configurations having the cyclic group lying flat over the Au chains (structure A) offer more stability than alternatives with positive tilt angle (structure B). The latter is energetically comparable, however, with adsorption at the Si honeycomb atoms (structure C). In this case, the Si=Si double bonds break in order to form a covalent bond with the sulfur atom, and one Si atom recovers an sp^3 hybridization. In contrast, the energies for adsorption, even partially, on Au (structures D and E) are small or even indicate an energy loss. We also considered a starting geometry with the TDT adsorbed parallel to the Au chain. During geometry relaxation the molecule was

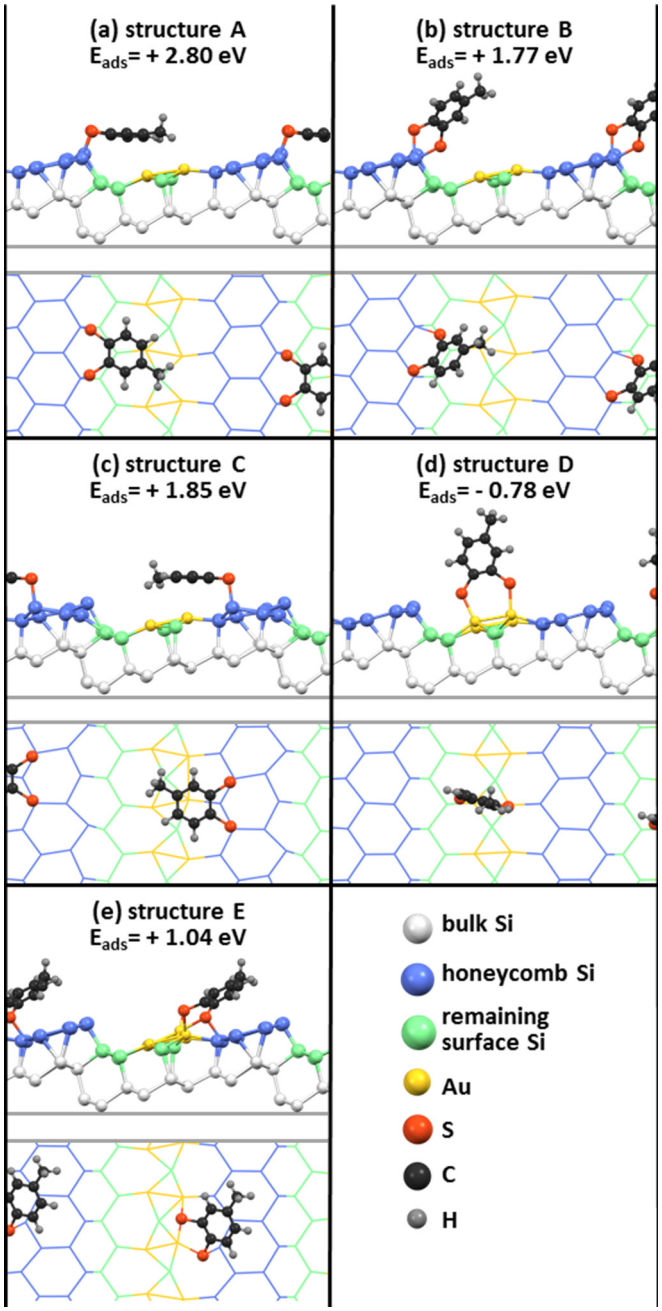

FIG. 4. Adsorption energies and geometries for dithiolate (TDT′) on the clean Si(553)-Au surface (top and side views).

found to "walk" across the chain and up the step edge [29], eventually remaining in geometry B. These results offer clear indications that adsorption at the Au chains is unfavored.

B. Geometry and energetics: Step-edge-passivated surface

We next consider TDT adsorption on the passivated Si(553)-Au:H surface. In this process, we assume that the surface has been prepared such that hydrogen passivates all step edge dangling bonds and then consider the adsorption of a TDT molecule on this passivated surface. For simplicity, we again follow the mechanism involved in channel (i) such that any H released through thiol dissociation forms molecular H_2 and

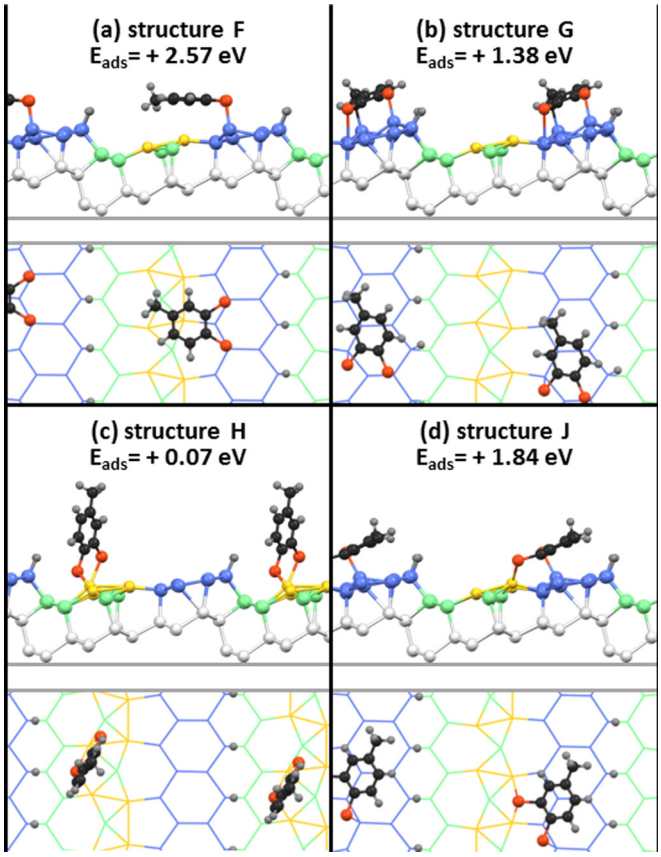

FIG. 5. Adsorption energies and geometries of dithiolate (TDT′) on Si(553)-Au with step edges passivated by hydrogen (top and side views). Color scheme is as in Figs. 3 and 4.

escapes to the rest gas. The adsorption energy of such a process [channel (iv)] is described by

$$E_{\mathrm{ads}}^{(\mathrm{iv})} = -\left(E_{(1\times4):4\mathrm{H}+\mathrm{TDT}'} + E_{\mathrm{H}_2} - E_{(1\times4):4\mathrm{H}} - E_{\mathrm{TDT}}\right). \quad (4)$$

Here (1 × 4):4H indicates the fully passivated surface, where all four dangling bond sites per cell are filled by hydrogen [compare with Eq. (3)]. Although it is tempting to compare the adsorption energies $E_{\mathrm{ads}}^{(\mathrm{iv})}$ calculated with this expression directly with the values of $E_{\mathrm{ads}}^{(\mathrm{i})}$ reported in the previous section using Eq. (1), that is not strictly allowed. To compare the two sets of adsorption energies, the chemical potential of the hydrogen reservoir μ_H should be considered instead of simply $1/2E_{\mathrm{H}_2}$, and conditions for high and low values of μ_H should be taken into account. Thus, Eq. (4) should be used only to compare the energies for different adsorption sites of TDT.

Geometries and adsorption energies are shown in Fig. 5. Guided by the results of Sec. III A we again consider adsorption at the more stable honeycomb sites (F and G) as well as sites on (H) or near (J) the Au chain. Now that the step edge is not available for TDT adsorption, the most stable site is at the honeycomb, parallel to the step edge, with the TDT molecule aligned almost parallel to the surface over the Au chains (F). The bonding mechanism (via strong S–Si bonds) is clearly comparable to structure C on the clean surface, which was also highly favored. Perpendicular orientation on the honeycomb chain (G) is less stable. Again, adsorption on the

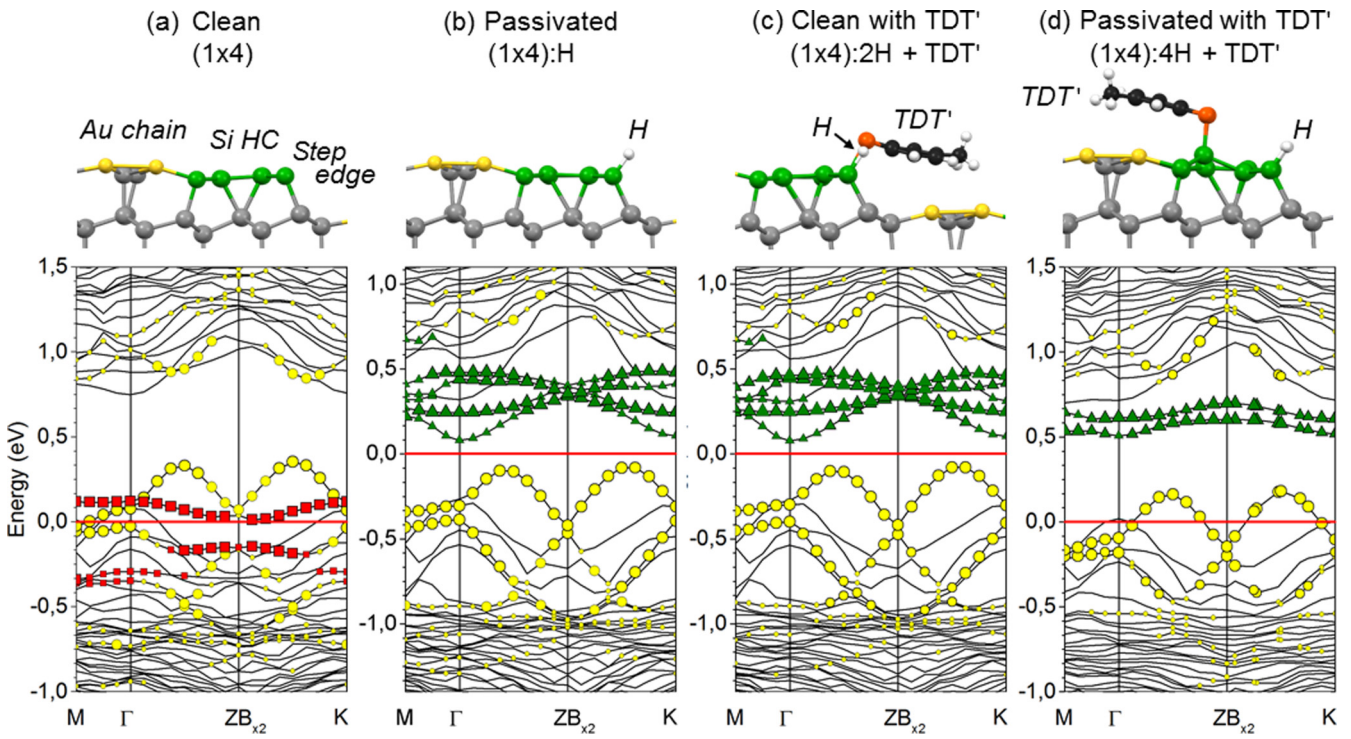

FIG. 6. Band structures of Si(553)-Au with various adsorbates. (a) Clean surface. (b) Following step edge passivation by hydrogen. (c) Clean surface with adsorbed thiolate (TDT′), following channel (ii), i.e., with step edge also passivated by two H atoms. (d) Step-edge-passivated surface with TDT′ adsorbed on the Si honeycomb, following channel (iv). In the band structures, yellow circles indicate Au states, red squares indicate states of Si atoms at the step edge, and green triangles are from doubly bonded Si atoms in the honeycomb stripe.

Au chain (H) is totally unfavored. This is in agreement with the total-energy pattern in Fig. 2(b), where we demonstrated that thiol adsorption on Au chains on the passivated Si(553)-Au:H surface is unlikely, in contrast to clean Au surfaces [6,8]. The energy gain significantly increases, however, when one of the S–Au bonding sites is replaced by a S–Si bond with a HC Si atom close to the Au chain (J).

C. Surface electronic structure

We now investigate the effects of TDT adsorption on the electronic structures of the clean and passivated Si(553)-Au surfaces. In each case we focus on the lowest-energy configurations. The band structure of the clean surface is displayed in Fig. 6(a). Bands associated with the step edge dangling bonds and the double Au chains are highlighted. As both bands cross the Fermi level, they are partially filled and therefore determine the surface metallicity. Figure 6(b) instead shows the computed band structure of the (step edge) passivated surface. Dangling-bond states at the step edge are completely filled and are shifted to lower energies (outside the energy range shown). Empty p_z-like states located at the Si honeycombs appear below the conduction band. Furthermore, the partially filled Au bonds also become completely filled, unpinning the Fermi level. Thus, passivation of the step edge with hydrogen actually makes the surface insulating, through a redistribution of charge from the dangling bonds to the Au chains. Our findings are in line with results from previous works [24,27].

Figure 6(c) reports the electronic structure of the surface following TDT adsorption via channel (ii) [see Fig. 3(b)], i.e., bonding of the molecule to the step edge through formation of S–Si bonds, dissociation of the –SH thiol groups, and passivation of the remaining two Si dangling bonds per cell with the liberated hydrogen. The resulting (insulating) band structure appears identical to that shown in Fig. 6(b). This indicates that the charge transfer from the TDT through S–Si bonding is equivalent to the charge transfer from atomic hydrogen through H-Si bonding, and no further charge redistribution within the molecule is involved. This is consistent with the similar electronegativities of S (2.5) and H (2.1). As before, the surface charge is redistributed so that the states associated with the Au chains are completely filled.

Last, Fig. 6(d) shows the band structure for TDT adsorption on the passivated surface, by means of channel (iv). This geometry corresponds to structure F in Fig. 5(a) and represents the lowest-energy configuration: adsorption of TDT on the honeycomb terrace sites. In this case, the surface recovers metallicity as the Fermi level passes once again through the bands of the Au chains. The TDT molecule causes two Si=Si double bonds [30] in the honeycomb chain to break. The rehybridized sp^3-like Si atoms in the honeycomb form covalent bonds with the sulfur atoms in the ligands. This local disruption of the honeycomb states is reflected in the electronic structure, which shows half of the unoccupied π^* states (triangles) disappearing deep into the occupied state manifold after TDT adsorption. To accommodate the new Si–Si bonds on the terraces, charge is drawn from the Au chains, rendering them metallic. Charge is not, however, transferred to the TDT molecule. The remaining two conduction bands associated with the Si honeycombs appear less dispersive than

before and follow the new (1 × 4) superperiodicity induced by the molecules.

Thus, even though the Au chains do not tend to directly bond with the TDT molecule, they are found to play a key role in determining the surface adsorption sites (as well as stabilizing the vicinal surface itself). On the (metallic) clean surface, they accept excess charge generated by covalent bonding of S (or H) to the partially filled dangling bonds at the step edge. On the (insulating) passivated surface, they donate charge in order to facilitate terrace adsorption via breaking of the stable honeycomb stripes. This ability of the double Au chains to act as a "charge reservoir" (via changes in the Au–Au dimerization distance) has been noted elsewhere [27,31]. The switch in role from acceptor to donor was induced in this case by externally passivating the step edge states with atomic hydrogen, i.e., without directly perturbing the chains themselves.

Further modification of the surface properties (adsorption sites, metallicity) could thus be controlled by additional doping (through additional physisorption or codoping or by exploiting energetically less favorable adsorption sites). Filling the Au-chain-related valence bands could lead to an organic-inorganic hybrid semiconducting surface with flat conduction bands associated with the honeycomb stripes. The adsorption of TDT on the honeycombs of the hydrogen-passivated surface results in two flat bands at ≈0.5 eV above the Fermi level, corresponding to collective states of electrons in the Si honeycomb double bonds that are unaffected by TDT adsorption. This opens a one-dimensional conducting channel with high electron mobility. Thus, TDT adsorption allows us to tailor the conduction of the one-dimensional chain structures. By controlling the edge passivation, insulating or conducting chains are made possible.

V. SUMMARY AND CONCLUSIONS

By means of DFT we have investigated the adsorption of TDT molecules on clean and H-passivated Si(553)-Au surfaces. In contrast to common expectations, adsorption via S–Au bonds is energetically unfavorable; we found that the Si dangling bonds at the edges are far more reactive. Following H passivation of the Si edge states, adsorption tends to occur through bonding to Si atoms in the honeycomb stripe between the double Au chain and the step edge.

The structural and energetic results are explained by the behavior of the band structure of the clean Si(553)-Au surface. Our work demonstrates that modification of the clean and H-passivated surfaces by molecular adsorption tunes the electronic properties between metallic and insulating regimes. Organic functionalization via molecules with thiol side groups was proven to be an interesting tool to prepare 1D conduction channels on vicinal Si(111) surfaces.

Codoping the surface with hydrogen is shown to be a route towards controlling the adsorption site for organic molecules. For the case of the dithiol studied here, it also controls the molecular orientation within the surface plane. This process thus offers potential for tuning surface electric fields (alignment of surface dipoles) and/or chirality of the molecular adlayer. Various geometrical and electronic factors are important in determining the molecular site and orientation: (1) Adsorption of thiolate (not thiol) is favored via strong directional covalent bonds. (2) S–Si bonds are strongly favored over S–Au ones. (3) Geometries having the aromatic ring parallel to the surface are favored. (4) Orientations that leave the aromatic ring stacked over the Au chains, rather than over the honeycomb, are preferred, irrespective of the Au chain metallicity. (5) Molecular orientation is determined by the energetics of covalent bonding, not by intermolecular forces. (6) The intramolecular S–S distance matches well with the distance between adjacent adsorption sites along $[1\bar{1}0]$, suggesting that Si(hhk)-Au systems are, in general, a good template for SAM growth of organic molecules with dithiol ligands. (7) Adsorption of hydrogen from dissociated thiol groups at the step edge could be, however, a limiting factor in the growth of SAMs at the step edge.

We hope that the results presented here encourage experimental research in this direction for this system as well as for other nanostructured substrates and organic linkers.

ACKNOWLEDGMENTS

The authors acknowledge financial support from the Senatsverwaltung für Wirtschaft, Technologie und Forschung des Landes Berlin, the Ministerium für Innovation, Wissenschaft und Forschung des Landes Nordrhein-Westfalen, the Bundesministerium für Bildung und Forschung, and the Deutsche Forschungsgemeinschaft (FOR1700). The North-German Supercomputing Alliance (HLRN) and the CINECA award under the ISCRA initiative for providing high-performance computing resources and support that have contributed to the research results reported in this paper are also acknowledged. The support of Dr. C. Tuma from the Zuse Institut Berlin concerning technical and implementation aspects in making the code run on HLRN resources is gratefully noted. C.H. thanks Dr. S. Elliott for useful discussions. S.S. thanks the Ministry of Education and Science of the Russian Federation for the award of Grant No. 16.3871.2017/4.6 ("Picometre diagnostics of parameters of 3D atomic structure of nanomaterials on the basis of XANES spectroscopy").

APPENDIX: INFLUENCE OF EXCHANGE AND CORRELATION

We consider chemisorption of TDT on the step-edge-passivated Si(553)-Au surface at three different geometries, F, G, and J (see Fig. 4), and apply three different XC functionals: LDA; the generalized gradient approximation of Perdew, Burke, and Ernzerhof (PBE) [32]; and PBE with the semiempirical vdW correction of Grimme [33,34]. We note that the latter, while easy to implement in practical calculations, also tends to overestimate vdW correlation with respect to other vdW flavors [35,36]. The results are summarized in Table II. In each case, the benzene ring was found to tilt toward the surface, almost lying flat. From the energies and bond distances (not listed) it is clear that molecules are chemisorbed on both Si honeycomb stripes and Au chains for all three functionals. All functionals find the Si–HC site more favored by a large margin (<0.7 eV). As expected, PBE gives the weakest binding energies, while PBE-vdW gives the strongest. However, LDA yields intermediate results and even

TABLE II. Adsorption energies for TDT adsorption on the H-passivated surface calculated with different exchange-correlation functionals at a Si HC site (F and G) and a Au chain site (J; see Fig. 5). Energies are in eV.

Site	Orientation	PBE	LDA	PBE-vdW
F, HC	∥ step, over Au	2.33	2.57	3.53
G, HC	⊥ step, over HC	0.88	1.38	1.75
J, Au/Si	45°, over HC	1.04	1.84	2.11

approaches the PBE+vdW value for the Au chain site. The largest deviation occurs for the F structure, where the molecular ring is strongly tilted toward the surface when the semiempirical vdW is included. From these data we conclude that, while LDA yields consistently correct predictions regarding favored *sites and orientation*, the absolute error in E_{ads} may be of the order of several tenths of an eV due to poor treatment of the substrate-ring correlation; that is, the molecular *alignment* may be incorrect. This observation does not affect the general conclusions obtained within LDA in this work.

[1] W. Schmidt, K. Seino, M. Preuss, A. Hermann, F. Ortmann, and F. Bechstedt, Appl. Phys. A **85**, 387 (2006).

[2] W. J. I. DeBenedetti and Y. J. Chabal, J. Vac. Sci. Technol. A **31**, 050826 (2013).

[3] D. Aswal, S. Lenfant, D. Guerin, J. Yakhmi, and D. Vuillaume, Anal. Chim. Acta **568**, 84 (2006).

[4] K. R. Rusimova and P. A. Sloan, Nanotechnology **28**, 054002 (2017).

[5] F. Costanzo, C. Sbraccia, P. L. Silvestrelli, and F. Ancilotto, Surf. Sci. **566**, 971 (2004).

[6] S. Franzen, Chem. Phys. Lett. **381**, 315 (2003).

[7] J. Ossowski, J. Rysz, M. Krawiec, D. Maciazek, Z. Postawa, A. Terfort, and P. Cyganik, Angew. Chem., Int. Ed. **54**, 1336 (2015).

[8] B. Höffling, F. Ortmann, K. Hannewald, and F. Bechstedt, Phys. Rev. B **81**, 045407 (2010).

[9] F. J. Himpsel, J. L. McChesney, J. N. Crain, A. Kirakosian, V. Pérez-Dieste, N. L. Abbott, Y.-y. Luk, P. F. Nealey, and D. Y. Petrovykh, J. Phys. Chem. B **108**, 14484 (2004).

[10] S. G. Kwon and M. H. Kang, Phys. Rev. Lett. **113**, 086101 (2014).

[11] S. C. Erwin and F. J. Himpsel, Nat. Commun. **1**, 58 (2010).

[12] P. C. Snijders and H. H. Weitering, Rev. Mod. Phys. **82**, 307 (2010).

[13] F. Zheng, I. Barke, X. Liu, and F. J. Himpsel, Nanotechnology **19**, 445303 (2008).

[14] J. N. Crain, J. L. McChesney, F. Zheng, M. C. Gallagher, P. C. Snijders, M. Bissen, C. Gundelach, S. C. Erwin, and F. J. Himpsel, Phys. Rev. B **69**, 125401 (2004).

[15] J. Aulbach, J. Schäfer, S. C. Erwin, S. Meyer, C. Loho, J. Settelein, and R. Claessen, Phys. Rev. Lett. **111**, 137203 (2013).

[16] J. Kautz, V. Janssen, R. Tromp, and S. van der Molen, Surf. Sci. **632**, L18 (2015).

[17] P. Nita, M. Jałochowski, M. Krawiec, and A. Stepniak, Phys. Rev. Lett. **107**, 026101 (2011).

[18] F. Edler, I. Miccoli, J. P. Stöckmann, H. Pfnür, C. Braun, S. Neufeld, S. Sanna, W. G. Schmidt, and C. Tegenkamp, Phys. Rev. B **95**, 125409 (2017).

[19] W. Kohn and L. J. Sham, Phys. Rev. **140**, A1133 (1965).

[20] P. Hohenberg and W. Kohn, Phys. Rev. **136**, B864 (1964).

[21] P. Giannozzi, S. Baroni, N. Bonini, M. Calandra, R. Car, C. Cavazzoni, D. Ceresoli, G. L. Chiarotti, M. Cococcioni, I. Dabo, A. Dal Corso, S. de Gironcoli, S. Fabris, G. Fratesi, R. Gebauer, U. Gerstmann, C. Gougoussis, A. Kokalj, M. Lazzeri, L. Martin-Samos, N. Marzari, F. Mauri, R. Mazzarello, S. Paolini, A. Pasquarello, L. Paulatto, C. Sbraccia, S. Scandolo, G. Sclauzero, A. P. Seitsonen, A. Smogunov, P. Umari, and R. M. Wentzcovitch, J. Phys. Condens. Matter **21**, 395502 (2009).

[22] J. Nocedal and S. J. Wright, *Numerical Optimization* (Springer, Berlin 2006), p. 664.

[23] F. Bechstedt, *Principles of Surface Physics* (Springer, Berlin, 2003).

[24] M. Krawiec, Phys. Rev. B **81**, 115436 (2010).

[25] J. P. Perdew and A. Zunger, Phys. Rev. B **23**, 5048 (1981).

[26] M. Krawiec and M. Jałochowski, Phys. Rev. B **87**, 075445 (2013).

[27] C. Hogan, E. Speiser, S. Chandola, S. Suchkova, J. Aulbach, J. Schäfer, S. Meyer, R. Claessen, and N. Esser (unpublished).

[28] J. Meyer, T. Bredow, C. Tegenkamp, and H. Pfnür, J. Chem. Phys. **125**, 194705 (2006).

[29] See Supplemental Material at http://link.aps.org/supplemental/10.1103/PhysRevB.97.045417 for an animation showing preferential adsorption of toluene-3,4-dithiolate at the step edge dangling bonds.

[30] S. C. Erwin and H. H. Weitering, Phys. Rev. Lett. **81**, 2296 (1998).

[31] J. Aulbach, S. C. Erwin, R. Claessen, and J. Schäfer, Nano Lett. **16**, 2698 (2016).

[32] J. P. Perdew, K. Burke, and M. Ernzerhof, Phys. Rev. Lett. **77**, 3865 (1996).

[33] S. Grimme, J. Comput. Chem. **25**, 1463 (2004).

[34] S. Grimme, J. Comput. Chem. **27**, 1787 (2006).

[35] T. Björkman, A. Gulans, A. V. Krasheninnikov, and R. M. Nieminen, J. Phys. Condens. Matter **24**, 424218 (2012).

[36] Y. Maimaiti and S. D. Elliott, J. Phys. Chem. C **119**, 9375 (2015).